Journal of Biotechnology 343 (2022) 47–51

Contents lists available at ScienceDirect

Journal of Biotechnology

journal homepage: www.elsevier.com/locate/jbiotec

Silver nanoparticles from residual biomass: Biosynthesis, characterization and antimicrobial activity

Pâmela Cristine Ladwig Muraro [a], Lailla Daianna Soltau Missio Pinheiro [a], Gabriela Chuy [a], Bruno Stefanello Vizzotto [a], Giovani Pavoski [b], Denise Crocce Romano Espinosa [b], Virginia Cielo Rech [a], William Leonardo da Silva [a,*]

[a] Nanoscience Graduate Program, Universidade Franciscana, Santa Maria, RS, Brazil
[b] Polytechnical School of Chemical Engineering, Universidade de São Paulo, São Paulo, SP, Brazil

ARTICLE INFO

Keywords:
Environmental impact
Aloe vera
Green nanotechnology
Nanomaterials

ABSTRACT

The industrial effluent contaminated with organic pollutants has been causing an increase in the toxicity of the ecosystem, causing a great environmental impact. Thus, the present work aims the green synthesis of silver nanoparticles (AgNPs) from Aloe vera, its characterization and antimicrobial activity against Pseudomonas aeruginosa (ATCC 27853) and Staphylococcus aureus (ATCC 25923). AgNPs were characterized by X-ray diffraction (XRD), Scanning Electronic Microscopy with Energy Dispersive Spectroscopy (SEM-EDS), Zeta Potential (ZP) and N_2 porosimetry (BET/BJH method). Antimicrobial activity were carried out by Minimal Inhibitory Concentration (MIC) method. The XRD demonstrated characteristic peaks of AgNPs at 38.29°; 44.55° and 64.81°, and SEM-EDS micrographs showed that AgNPs produced by biomolecules of Aloe vera extract resulted in a weight concentration around 92.59% silver, 7.15% oxygen and 0.26% chlorine. Regarding zeta potential, all samples showed negative electric charge (around −35.3 mV), while N_2 porosimetry resulted in a surface specific area of 6.09 $m^2\ g^{-1}$, with a volume and diameter pore of 0.032 $cm^3\ g^{-1}$ and 33.47, respectively. Antimicrobial activity was observed at 15.62 μg mL^{-1} and 31.25 μg mL^{-1} for P. aeruginosa and S. aureus, respectively. Thus, AgNPs can be considered a promising nanoparticle for degradation of organic pollutants in aqueous solution as well as an adjuvant for treatment of microbial infections.

1. Introduction

Industrial wastewater is characterized by the diversity of its chemical composition, ranging from inorganic and organic compounds, such as toxic and recalcitrant pollutants (Ferreira-Leitão et al., 2010), which can change natural ecosystems, causing contamination in all ecosystems, becoming an environmental liability (Bernabeu et al., 2011). Moreover, wastewater treatment plants (WWTPs) can result in great environmental impact caused by the inadequate treatment of wastewater and the generation of anthropogenic waste and by-products (Chen et al., 2013; Soon and Hameed, 2011).

In addition, some of the main pollutants in the aquatic environment come from industries that use dyes in their production processes, such as textiles, leather, paper and plastics, since they consume a large volume of water, generating a significant amount of colored wastewater (Rafatullah et al., 2010). Thus, most dyes cause change to the environment, as they cause visual pollution and the modification of biological cycles, affecting the aquatic environment and impairing photosynthesis processes (Zanoni and Carneiro, 2001).

Nanobiotechnology is an area of knowledge that integrates several areas of knowledge, such as physics, chemistry, biology and materials science. Nanoparticles, due to their nanoscale size (10^{-9} m), present new or improved properties based on their specific characteristics (size, distribution, morphology, phase and composition, mainly) when compared to macro and microparticles from the same source (Resende, 2017).

Green nanotechnology focuses on the relationship with sustainability through methods and materials that aim to generate products with reduced environmental impact associated with economic and social areas, such as green nanocatalysts and green nanoparticle (Narayanan and Sakthivel, 2011). This concept offers opportunities regarding the use of biomolecules or metabolites during the synthesis routes of green

* Corresponding author.
E-mail address: w.silva@ufn.edu.br (W.L. da Silva).

https://doi.org/10.1016/j.jbiotec.2021.11.003
Received 27 May 2021; Accepted 3 November 2021
Available online 23 November 2021
0168-1656/Published by Elsevier B.V.

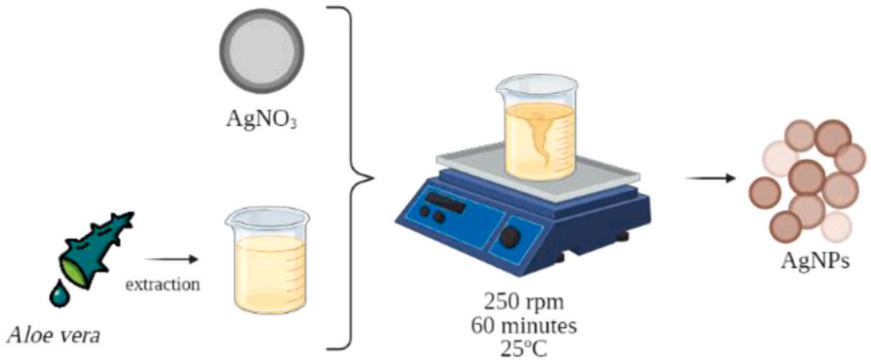

Fig. 1. Experimental scheme of the synthesis of AgNPs. Negative control. **PC:** Positive control. **3–12**: AgNPs concentrations ranging from 500 mg mL^{-1} to 0.98 mg mL^{-1}. * *P. aeruginosa*. # *S. aureus*.

nanoparticles, because these materials are available with a wide application and specific characteristics, such as biodegradability and biocompatibility (Da Silva et al., 2017).

For example, plants produce a range of metabolites that can act synergistically in reduce metallic ions and/or stabilize metallic nanoparticles (Akhtar et al., 2013). Moreover, plants and derivatives are known for antimicrobial properties and have long been used as therapeutic agents to treat various infections (Akhtar et al., 2013). Thus, these properties can be attributed to the presence of a series of secondary metabolites, such as flavonoids, alkaloids, phenols and terpenoids (Hussain and El-Anssary, 2019).

In this context, this present work aims the green synthesis, characterization and determination of the antimicrobial activity of silver nanoparticles (AgNPs) obtained from Aloe vera extract.

2. Materials and methods

2.1. Preparation of Aloe vera extract

The preparation of the Aloe vera extract was according to the literature (Chandran et al., 2006), where 30 g of the gel were chopped into small strips and magnetic stirring for 30 min in 1000 mL of distilled water at room temperature (25 ± 2ºC).

2.2. AgNPs biosynthesis

According to the literature, a chemical reduction method was used, according to the literature was used for the biosynthesis of silver nanoparticles (Chandran et al., 2006). Thus, 5 mL of Aloe vera extract with 5 mL of $AgNO_3$ (10^{-2} mol L^{-1}, 99.9%, Sigma Aldrich) and 2.5 mL of ammonium hydroxide (30%, P.A., Sigma Aldrich) were placed under magnetic stirring (60 min/ 250 rpm) at ambient temperature (25 ± 2ºC). After, the solution was collected and dried (De Leo, universal model) at 80 ºC for 12 h. Fig. 1 shows the schematic representation of the AgNPs biosynthesis.

2.3. Characterization techniques

For the zeta potential measurements (ZP), Malvern-Zetasizer® model nanoZS (ZEN3600, United Kingdom) with closed capillary cells (DTS 1060) (Malvern, United Kingdom) was used to measure the surface charge values of the samples. Scanning electron microscopy (SEM) with energy dispersive spectroscopy (EDS) was used to determined the morphological characteristic of the silver nanoparticle was used with Phenom Prox Scanning Electron Microscope (Thermo Fisher Scientific). XRD was used for the identification of crystalline phases using Bruker diffractometer, model D2 Advance, with copper tube ($K_{Cu-\alpha}$ radiation =

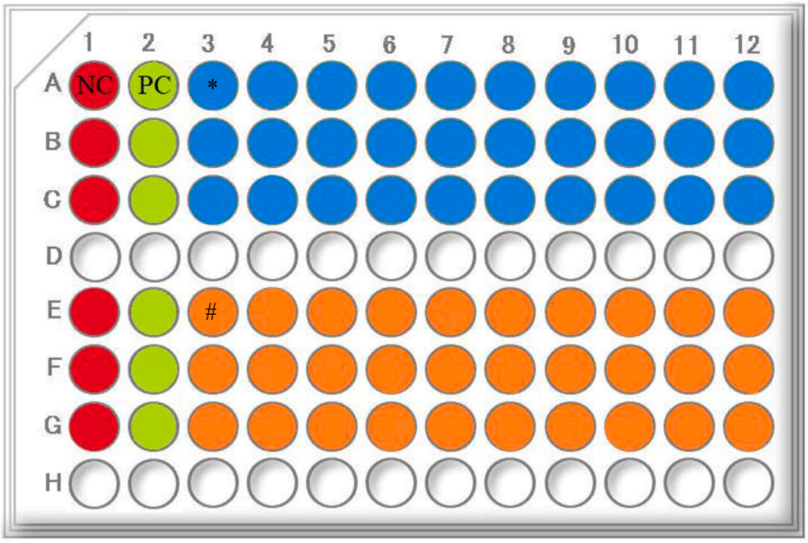

Negative control. **PC:** Positive control. **3-12**: AgNPs concentrations ranging from 500 mg mL^{-1} to 0.98 mg mL^{-1}. * *P. aeruginosa*. # *S. aureus*.

Fig. 2. Representation of the AgNPs distribution using the microdilution method.

Table 1
Surface area (S_{BET}), pore volume (Vp), pore diameter (Dp) and zeta potential (ZP) of AgNPs.

Sample	S_{BET} ($m^2\ g^{-1}$)	Vp ($cm^3\ g^{-1}$)	Dp (nm)	ZP (mV)
AgNPs	6.09 ± 0.05	0.032 ± 0.03	33.47 ± 0.04	-35.3

1.5418 Á) ranged 10º to 70º, with acceleration voltage and applied current of 30 kV and 30 mA, respectively. N_2 adsorption/desorption was used to determine the specific area (S_{BET}) and porosimetry (diameter and volume pore) by the Brunauer-Emmett-Teller Equation (BET Method) and Barret-Joyner Equation -Halenda (BJH Method) (Brunauer and Emmett, 1937), respectively, in the range of P Po^{-1} = 0.05–0.35. Thus, the samples (100–200 mg) were degassed at a pressure of 10^{-2} mbar with a temperature of 120 ºC for 12 h, in ASAP 2020 Plus Micromeritics equipment. In order to verify the possible sustainable applicability of the AgNPs, minimum inhibitory concentration (MIC) of AgNPs were performed against S. aureus ATCC 25923 and P. aeruginosa ATCC 27853 strains by broth microdilution method using 96-well polystyrene microplates (Clinical and Laboratory Standards Institute, 2018). The assay was repeated three times (each tested well in triplicate) using a stock solution of AgNPs diluted in sterile distilled water at a

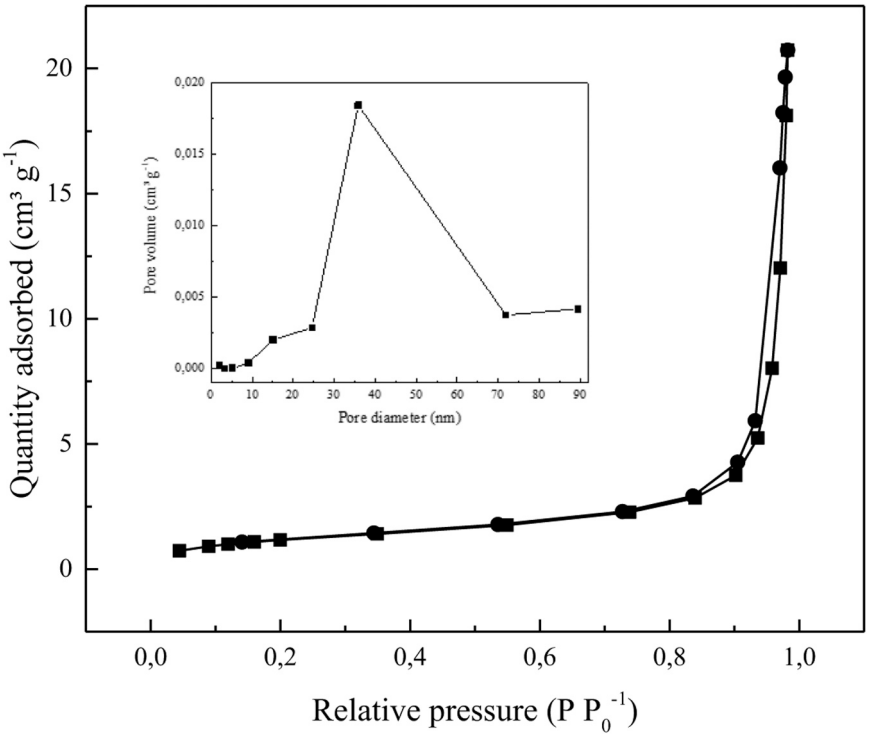

Fig. 3. Isotherms for N_2 adsorption/desorption of the AgNPs. In detail: the distribution of the pore volume of the same system.

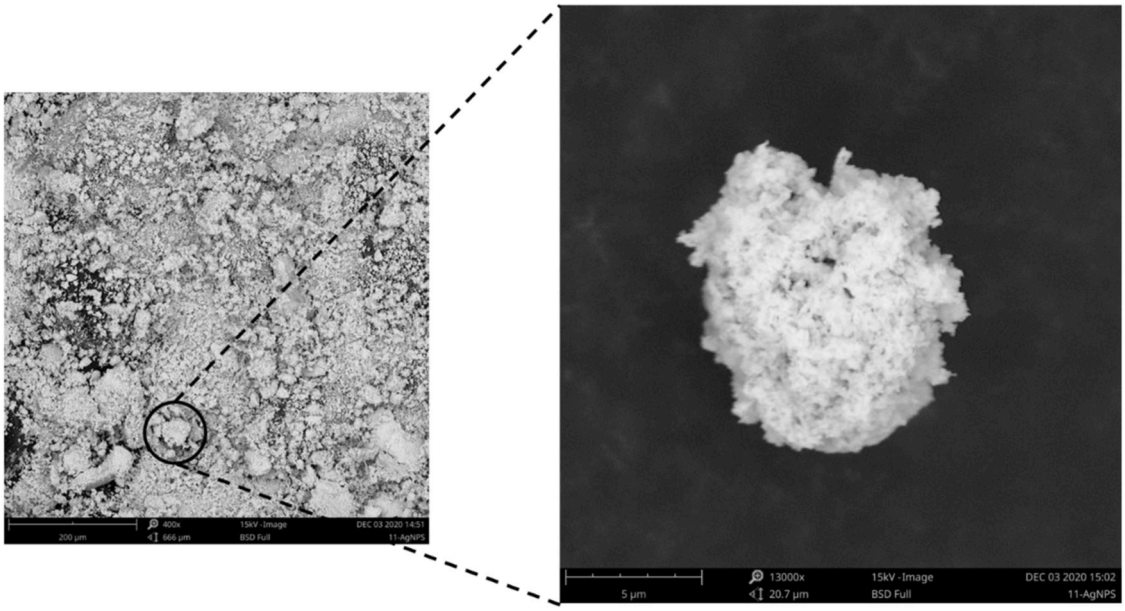

Fig. 4. . SEM micrographs of silver nanoparticles (AgNPs).

Table 2
Chemical composition of AgNPs.

Sample	Elements – Weight concentration		
	Ag (%)	O (%)	Cl (%)
AgNPs	92.59	7.15	0.26

Table 3
MIC values (μg mL^{-1}) of the silver nanoparticles (AgNPs).

Sample	MIC (μg mL^{-1})	
	Staphylococcus aureus ATCC 25923	*Pseudomonas aeruginosa* ATCC 27853
AgNPs	15.62	7.81

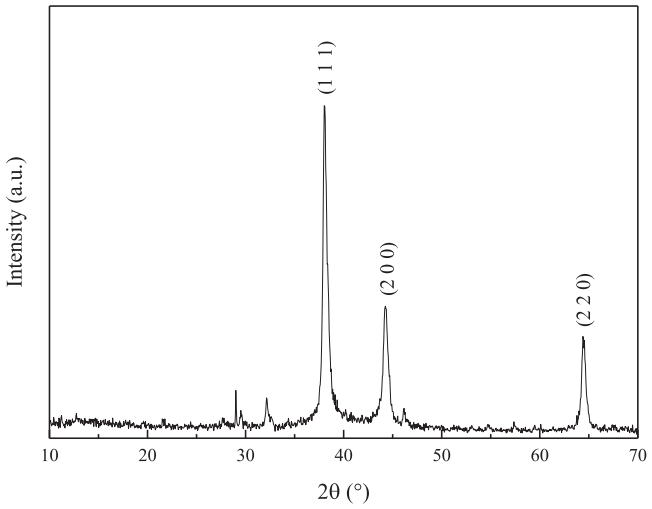

Fig. 5. . X-ray patters of silver nanoparticles (AgNPs).

concentration of 500 mg mL^{-1}. First, 100 μL of Mueller Hinton broth (MH, Sigma Aldrich®) were added to each well on the plate, followed by the addiction of 100 μL of the AgNPs stock solution at the third column, transferring 100 μL to the adjacent columns, performing a serial dilution of 1:2 w/w (250 mg mL^{-1} to 0.48 mg mL^{-1}). Afterwards, 10 μL of bacterial inoculums (1×10^4 CFU mL^{-1}) were added to each well, minus negative control column (contamination control) which received 10 μL of distilled water. For the positive control column, only MH broth and bacterial inoculum were inoculated, to check for bacterial viability. Thus, microplates were incubated for 18–24 h at 37 ± 2 °C. After this incubation, 20 μL of 5% (w/w) triphenyl tetrazolium chloride (TTC) solution was added to each well, and the plates were reincubated for another 2 h at 37 ± 2 °C. Plates were read visually, where the color changed from colorless to red which indicates bacterial growth, with MIC value defined as the lowest concentration (mg L^{-1}) of the AgNPs responsible for preventing bacterial growth. According to Fig. 2.

3. Results and discussion

3.1. Characterization techniques

Table 1 shows the results of N_2 porosimetry and zeta potential, where AgNPs showed S_{BET} of 6.09 m^2 g^{-1}, in relation to the pore volume it obtained a total of 0.032 cm^3 g^{-1}. In addition, AgNPs showed a negative charge surface potential, according to zeta potential, indicating load compatibility with cationic organic pollutants. Fig. 3 shows the typical isotherms of N_2 adsorption/desorption of AgNPs and the pore size distribution curves.

According to Table 1, pore diameter (Dp) of silver nanoparticle showed a mesoporous characteristic ($2 < Dp < 50$ nm) according to Thommes and collaborators (2015). Fig. 3 showed that the N_2 adsorption/desorption isotherms of the AgNPs are characterized by type V isotherms typical of mesoporous materials, with multilayer filling (McCusker et al., 2001). Hysteresis curve is of H1 type, commonly observed in porous materials characterized by consisting of agglomerates or compacted uniform spheres, in the form of cylinders with open ends (Thommes et al., 2015).

Fig. 4 shows the micrographs of AgNPs, where it was possible to identify a heterogeneous surface with small agglomerations of nanoparticles without a well-defined morphology. The appearance of

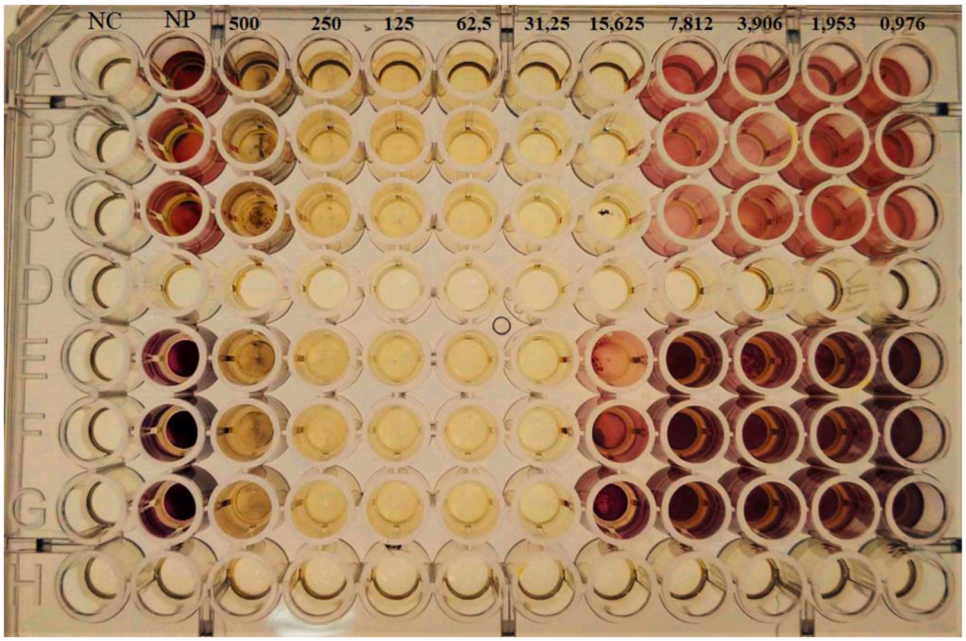

Fig. 6. MIC results of AgNPs tested against P. aeruginosa and S. aureus.

secondary metabolites in the extract of Aloe vera may be responsible for this aggregation (Singh et al., 2021). Cluster size was measured using ImageJ software (NIH, USA) and resulted in a size of approximately 9.71 μm. In addition, Tables 2 and 3 shows EDS results found for AgNPs, demonstrating that the nanoparticles present a weight concentration around of 92.59% silver, 7.15% oxygen and 0.26% chlorine. The presence of these elements in small quantities may be due to the biomolecules of Aloe vera extract used as a reducing agent.

Fig. 5 shows the diffractogram of the AgNPs, where it was possible to identify the characteristic peaks of AgNPs at 38.29°; 44.55° and 64.81° corresponding to the planes (111), (200), (220) respectively, according to ICDD (database #04-0783 card number). The peaks 32.09°; 44.19° and 64.55° correspond to $AgNO_3$, which was not reduced consequently remaining in the sample in a small amount (Mehta et al., 2017).

The standard Debye–Scherer equation was used to determine the average particle size of Ag NPs and is given by (Cullity, 1956) (Eq. 1):

$$d = \frac{0.9\lambda}{\beta cos(\theta)} \quad (1)$$

Where, k is the incident X-ray wavelength, b = full width at half maxima (FWHM) of the peak and h is the Bragg diffraction angle. The average particle size was determined around 20.9 nm.

3.2. Antimicrobial activity

Fig. 6 shows the antimicrobial activity against P. aeruginosa and S. aureus, where it was possible to verify that the first pathogen presented a higher sensitivity in relation to the second, since the MIC of the nanoparticle was 15.62 μg mL^{-1} and 31,25 μg mL^{-1} respectively. Gram-negative bacteria have an outer membrane, composed of proteins, lipopolysaccharides and phospholipids, followed by a thin layer of peptidoglycan (~ 10 nm), while gram-positive bacteria have a thick layer of peptidoglycan (~ 20–80 nm) and are devoid of outer membrane (Milton and Kwang-Shin, 2014), allied to the presence of negatively charged teichoic acids at the cell wall which can repel the binding of the AgNPs, difficulting its cell wall penetration, thus justifying a greater activity in P. aeruginosa compared to S. aureus. Moreover, the reduced size of the nanoparticle obtained contributes to a larger surface area of interaction, which results in higher antimicrobial activity (Peiris et al., 2017).

4. Conclusions

According with this study, it was possible to verify the success of AgNPs synthesis from Aloe vera extract, acting as a reducing agent by the method of chemical reduction. The average size of the nanoparticles calculated by the size of the lens was approximately 20.9 nm, determined by the Debye-Scherrer equation. SEM showed small clusters of AgNPs with an average size of 9 μm, and EDS showed a significant weight concentration of silver in green nanoparticles. In addition, AgNPs showed good activity against P. aeruginosa and S. aureus, indicating its use as an antimicrobial agent.

Acknowledgments

We thank the Polytechnical School of Chemical Engineering at University of São Paulo (USP, Brazil – SP) and Franciscan University (UFN, Brazil – RS) for the support and assistance to carry out the present work. This work received financial support from the Foundation for Research of the State of Rio Grande do Sul (FAPERGS–Project 19/2551-0001606-9).

Declaration of competing interest

The authors declare that they have no known competing financial interests or personal relationships that could have influenced the work reported in this paper.

References

Akhtar, M.S., Panwar, J., Yun, Y., 2013. Biogenic synthesis of metallic nanoparticles by plant extracts. ACS Sustain. Chem. Eng. 1 (6), 591–602.
Bernabeu, A., Vercher, R.F., Santos-Juanes, L., Simón, P.J., Lardín, C., Martínez, M.A., Vicente, M.A., González, R., Llosá, C., Arques, A., Amat, A.M., 2011. Solar photocatalysis as a tertiary treatment to remove emerging pollutants from wastewater treatment plant effluents. Catal. Today 161 (1), 235–240.
Brunauer, S., Emmett, P.H., 1937. The use of low temperature van der Waals adsorption isotherms in determining the surface areas of various adsorbents. J. Am. Chem. Soc. 59 (12), 2682–2689.
Chandran, S.P., Chaudhary, M., Pasricha, R., Ahmad, A., Sastry, M., 2006. Synthesis of gold nanotriangles and silver nanoparticles using *Aloe vera* plant extract. Biotechnol. Prog. 22 (2), 577–583.
Chen, Q., Ji, F., Liu, T., Yan, P., Guan, W., Xu, X., 2013. Synergistic effect of bifunctional Co–TiO_2 catalyst on degradation of Rhodamine B: Fenton-photo hybrid process. Chem. Eng. J. 229, 57–65.
Clinical And Laboratory Standards Institute (2018) Methods for dilution antimicrobial susceptibility tests for bacteria that grow aerobically. Approved standard–Seventh edition: M07-A09. 32(2).
Cullity, B.D., 1956. Elements of X-ray Diffraction. Addison-Wesley Publishing Inc, United States.
Da Silva, L.P., Bonatto, C.C., Pereira, F.D.E.S., Silva, L.D., Albernaz, V.L., Polez, V.L.P., 2017. Green Nanotechnology for Synthesis of Metal Nanoparticles. Blucher, São Paulo, pp. 967–1012.
Ferreira-Leitão, V., Gottschalk, L.M.F., Ferrara, M.A., Nepomuceno, A.L., Molinari, H.B. C., Bon, E.P., 2010. Biomass residues in Brazil: availability and potential uses. Waste Biomass Valoriz. 1 (1), 65–76.
Hussain, R.A., El-Anssary, A., 2019. Plants secondary metabolites: the key drivers of the pharmacological actions of medicinal plants. Herbal Medicine, London.
McCusker, L.B., Liebau, F., Engelhardt, G., 2001. Nomenclature of structural and compositional characteristics of ordered microporous and mesoporous materials with inorganic hosts (IUPAC Recommendations 2001). Pure Appl. Chem. 73 (2), 381–394.
Mehta, B.K., Chhajlani, M., Shrivastava, B.D., 2017. Green synthesis of silver nanoparticles and their characterization by XRD. J. Phys. Conf. Ser. 836 (1), 012050.
Milton, R.J., Kwang-Shin, K. 2014. Medical Microbiology, fourth edition, Texas.
Narayanan, K.B., Sakthivel, N., 2011. Green synthesis of biogenic metal nanoparticles by terrestrial and aquatic phototrophic and heterotrophic eukaryotes and biocompatible agents. Adv. Colloid Interface Sci. 169 (2), 59–79.
Peiris, M.K., Gunasekara, C.P., Jayaweera, P.M., Arachchi, N.D., Fernando, N., 2017. Biosynthesized silver nanoparticles: are they effective antimicrobials? Mem. Inst. Oswaldo Cruz 112, 537–543.
Rafatullah, M., Sulaiman, O., Hashim, R., Ahmad, A., 2010. Adsorption of methylene blue on low-cost adsorbents: a review. J. Hazard. Mater. 177 (1–3), 70–80.
Resende, R.R., 2017. Biotechnology applied to agro & industry: fundamentals and applications, fourth edition, São Paulo.
Singh, J., Tripathi, J., Sharma, M., Nagar, S., Sharma, A., 2021. Study of structural, optical properties and antibacterial effects of silver nanoparticles synthesized by green synthesis method. Mater. Today 46, 2294–2297.
Soon, A.N., Hameed, B.H., 2011. Heterogeneous catalytic treatment of synthetic dyes in aqueous media using Fenton and photo-assisted Fenton process. Desalination 269 (1–3), 1–16.
Thommes, M., Kaneko, K., Neimark, A.V., Olivier, J.P., Rodriguez-Reinoso, F., Rouquerol, J., Sing, K.S., 2015. Physisorption of gases, with special reference to the evaluation of surface area and pore size distribution (IUPAC Technical Report). Pure Appl. Chem. 87 (9–10), 1051–1069.
Zanoni, M.V.B., Carneiro, P.A., 2001. Disposal of Textile Dyes. Ciência Hoje, pp. 61–71, 29(174).